Hydrodynamic Characterisation of Layered Herringbone Microchannels

Alberto CANTU-PEREZ[1], Simon BARRASS[1], Andreas FREITAG[2], Thomas DIETRICH[2], Asterios GAVRIILIDIS[1*]

* Corresponding author: Tel.: +44 (0)20 76793811; Fax: +44 (0)20 73832348; Email: a.gavriilidis@ucl.ac.uk
1: Chemical Engineering Department, University College London, UK
2: Mikroglas Chemtech GmbH, Mainz, Germany

Abstract The performance of a layered herringbone microstructured channel is compared with the staggered herringbone micromixer (SHM) originally proposed by Stroock *et al.* (2002). The layered configuration uses a single set of herringbone structures for two adjacent channels. Mixing and residence time distributions (RTDs) are studied both theoretically, via computational fluid dynamics and particle tracking algorithms, and experimentally. Experimental RTD measurements were performed by monitoring the concentration of a tracer dye by means of a LED-photodiode system. The proposed layered design gives similar results in terms of mixing and RTD as the standard SHM and it outperforms the behaviour of a rectangular channel.

Keywords: Residence time distribution, micromixing, microchannel, staggered herringbone micromixer.

1. Introduction

The use of miniaturised devices for applications in micro total analysis systems, lab-on-a-chip and chemical process technology is becoming increasingly widespread. Intensive research has been focused on microprocess technology due to its advantages compared to macroscopic equipment in terms of high heat and mass transfer. Conversion and selectivity in chemical reactions is strongly dependent on the degree of mixing and the residence time distribution (RTD) of the reactor. Usually a narrow RTD is preferred, as this would in principle be beneficial for both conversion and selectivity. The fluid flow in microchannels is laminar, thus mixing relies primarily on diffusion mechanisms rather than turbulence. A dimensionless number that compares convection over diffusion processes is the Peclet number, *Pe*:

$$Pe = \frac{Ud}{D} \qquad (1)$$

where U is the fluid velocity, d is the characteristic dimension (width) of the channel and D is diffusivity. For high Peclet numbers (typical for liquid flows) convection dominates the mixing process (Nguyen and Wu, 2005) and the mixing length in a microchannel is rather long. Furthermore, the RTD in plain microchannels at high Peclet numbers is characterised by an asymmetric profile which may negatively impact conversion and selectivity of a chemical reaction. Staggered herringbone micromixers (SHM) increase the contact area and decrease the diffusion path between the streams, achieving complete mixing in a much lower distance than a plain channel relying only on diffusion (Stroock *et al.*, 2002). Moreover, they help in narrowing the RTD.

In this work, a layered herringbone structured microchannel is investigated. This configuration is studied numerically with Comsol Multiphysics and Matlab in terms of mixing using particle tracking. In addition, both numerical simulations and experiments are carried out for RTD characterisation.

2. Geometry

The layered microchannel geometry considered in this work is shown in figure 1, while its dimensions are shown in table 1. It consists of two symmetric, top and bottom microchannels separated by a layer with etched-through herringbone grooves. It is important to note that the herringbones are not placed on the microchannel floor and the fluids flowing in top and bottom channels are able to communicate through these features. A schematic of one cycle of the layered herringbone design is shown in figure 1A, while figure 1B shows the chip fabricated in photo-structurable glass (FOTURAN) used in the experiments.

A

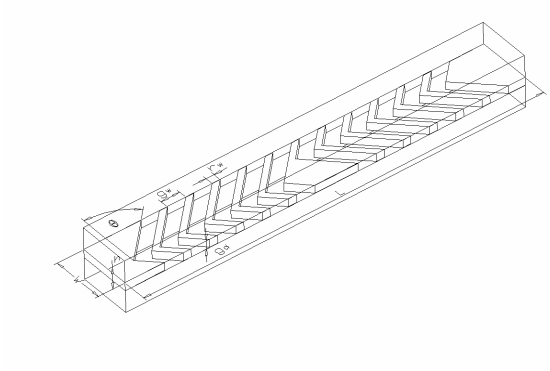

B

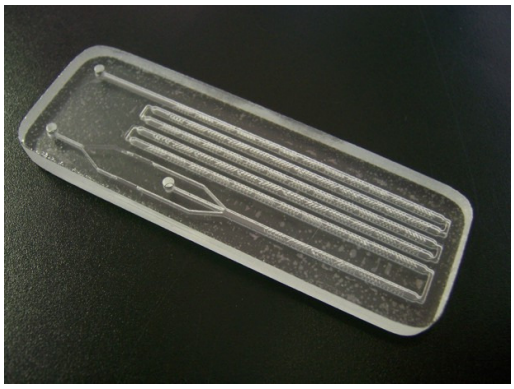

Figure 1. A) Schematic of one cycle of the layered herringbone channel. B) Picture of the glass chip employing a layered herringbone channel. The chip is 26x76mm.

Table 1. Dimensions of the different geometries studied.

	Layered herringbone	SHM	Rectangular channel
Width (w)	1.2 mm	200 μm	200 μm
Height (h)	510 μm (top, bottom channels)	85 μm	85 μm
Groove width (g_w)	300 μm	50 μm	-
Groove depth (g_d)	370 μm	31 μm	-
Ridge width (r_w)	300 μm	50 μm	-
Angle (θ)	45°	45°	-
Pe	10^4	10^4	10^4

3. Simulation Details

The Navier-Stokes and the continuity equations for the conservation of mass, equations (2) and (3) respectively, are solved simultaneously with the fluid dynamics module in COMSOL Multiphysics 3.5a. This software has been successfully used for the simulation of fluid flow in microchannels (Hassell and Zimmerman, 2006*;* Kee and Gavriilidis, 2008*;* Williams *et al.*, 2008).

$$\rho\frac{\partial v}{\partial t}-\nabla\cdot\left[\eta\left(\nabla v+(\nabla v)^T\right)\right]+\rho(v\cdot\nabla)v+\nabla p=0 \quad (2)$$

$$\nabla\cdot v=0 \quad (3)$$

where ρ is density, v is velocity field, η is dynamic viscosity, p is pressure, and t is time. The velocity field is solved using periodic boundary conditions so that the velocity at the outlet boundary is the same as the inlet one, with a constant flowrate throughout the channel. Additionally, non-slip boundary conditions are applied to all walls. A mesh consisting of 50,198 number of elements and 202,795 degrees of freedom is used to execute the simulations in Windows XP with Pentium IV 3.00 GHz CPU and 2 GB of RAM. At least 15% of the elements were placed inside the grooves. With these conditions the solution was found to be mesh independent. The solution is exported to MATLAB and a particle tracking algorithm with a random walk type diffusion step is used to obtain the positions of the particles by solving equation

(4) for a fixed time step. The positions of the particles are recorded and the procedure is repeated over a specified number of steps.

$$d\vec{x} = v\left(\vec{x}\right)dt + \sqrt{2Ddt}\,\xi \tag{4}$$

where $\vec{x}$ is the vector with the positions of the particles and ξ is a random number with zero mean and unit variance. It has been shown by Levenspiel and Turner (1970) that to obtain the correct RTD when the velocity profile after the injection and measurement point is not flat (for example in laminar flow) the number of particles introduced must be proportional to the velocity at each radial injection position and the measurement must be the mixing cup reading. For this reason 4400 particles are distributed proportionally to the axial velocity at the channel inlet. For mixing simulations a uniform distribution of the particles is used. The code is set so that the velocity field obtained for the first cycle could be used over many mixing cycles. A standard fourth order Runge-Kutta method with fixed time steps is used to obtain the solution. For the mixing simulations only the convective part of the particle tracking code is used (first term in equation (4)) which is valid in the limit of high Pe.

4. Methods

4.1 Mixing

Mixing is characterized by the nearest neighbour analysis method (Aubin *et al.*, 2005). In this method, the positions of the tracer particles after certain number of herringbone cycles are compared with the positions of particles distributed uniformly throughout the cross-section. By calculating the distances between the tracer particles and the particles in the uniform array, a measure of mixing can be calculated. The extent of mixing can be quantified by measuring the spatial distribution of the tracers in the cross-section. The tracers will be in a uniform array when the distances between the tracers and the particles in the uniform array are less or equal to the mean distance between the particles in the uniform grid. In this case the system is completely mixed. For other cases the degree of mixing can be thought as the percentage of tracers that are already arranged in a uniform manner, thus it is possible to calculate the mixing percentage as the ratio of particles arranged in uniform manner over the total number of particles. Experimental mixing evaluation was performed by a confocal fluorescence microscope. Acridine orange was used as the fluorescent dye.

4.2 Residence Time Distributions

Numerical RTDs are obtained by recording the number of particles arriving at the channel exit, N_i, as a function of time interval, $\Delta t_i = t_{i+1} - t_i$, with equation (5):

$$E(t_i) = \frac{N_i}{\sum_{i=1}^{n} N_i \Delta t_i} \tag{5}$$

The RTD in dimensionless form is obtained from:

$$E(\theta) = t_m E(t_i) \tag{6}$$

where t_m is:

$$t_m = \frac{\sum_{i=1}^{n} t_i N(t_i) \Delta t_i}{\sum_{i=1}^{n} N(t_i) \Delta t_i} \tag{7}$$

The variance of the distribution can be calculated as follows:

$$\sigma^2 = \frac{\sum_{i=1}^{n} (t_i - t_m)^2 E(t_i) \Delta t}{\sum_{i=1}^{n} E(t_i) \Delta t} \tag{8}$$

which in dimensionless form changes to:

$$\sigma_\theta^2 = \frac{\sigma^2}{t_m^2} \tag{9}$$

Experimental RTDs were obtained by injecting an inert tracer into the chip (figure 1) and recording its concentration at the outlet photometrically. An HPLC pump (Waters 510) was used for feeding deionized water to the chip (flowrate 1 ml/min). The tracer pulse (Parker Blue dye with calculated D=1.3x10^{-9} m^2/s) was introduced by a 6-port sample injection valve (Rheodyne) equipped with 5 µl sample loop and an internal position signal switch that indicates the time of injection. The tubing among all components was Teflon 0.254mm ID. Tracer detection was performed by light absorption. Illumination was provided by two square LEDs (Kingbright L-1553IDT). To make sure that only light going through the desired channel area was collected, black tape was used to mask the neighbouring areas. To isolate the system from ambient light it was placed in a dark box. The detection system was based on a linear diode array detector (TSL, 1401R-LF) which had 128 diodes. Data from the sensor was collected using a National instruments PCI-6010 data acquisition card before being analysed and displayed on a computer using a program written in Labview. Every 100 ms the computer would average the previous two scans, calculate the absorbance for each diode and display the result. The absorbance of the tracer dye was found to be in accordance with the Beer-Lambert law.

5. Results and Discussion

Figure 2A shows the distributions of the tracer particles over the cross-section of the channel for the SHM and the layered configuration after 5 herringbone cycles. The effect of diffusion was not considered in this simulation. Figure 2B shows the calculation of percentage of mixing as function of number of cycles via the nearest neighbour analysis as described in section 4.1. The layered herringbone channel gives qualitatively similar mixing results as the standard herringbone mixer (SHM). However, as can be seen in figure 2B, the layered herringbone microchannels have a slightly better performance than the standard SHM. This is due to the absence of the groove floor which eliminates the no-slip boundary condition, increasing the flowrate within the grooves. This is further supported by figure 2C which shows the velocity in the z coordinate (vertical axis) at the top channel/groove interface. Negative values indicate fluid going into the groove and positive ones fluid coming out of the groove. The figure shows that the layered herringbone configuration has a larger area with negative values (at the groove apex) with similar absolute numbers as the SHM. Furthermore, the regions of positive velocity for the layered herringbone are closer to the channel wall and are higher in magnitude than the ones for the SHM. This indicates that the layered herringbone induces stronger transverse movement than the SHM.

The numerical and experimental RTDs are shown in figure 3. It was found that there was disagreement for the average residence time between experiments and modelling. However, when the RTD is shown in dimensionless form (as in figure 3) the agreement between numerical and experimental data is good. Furthermore, the RTD for the layered herringbone microchannel is narrower compared to a rectangular channel of the same dimensions as demonstrated in figure 3.

Flow maldistribution was thought to be partly responsible for the disagreement between the measured and calculated mean residence times. Confocal fluorescence microscopy was used to investigate this further. Acridine orange and water were pumped to the two inlets of the chip at equal flowrates. The stream of acridine orange splitted in two and entered as two streams on the sides of the channel, while water entered through the middle.

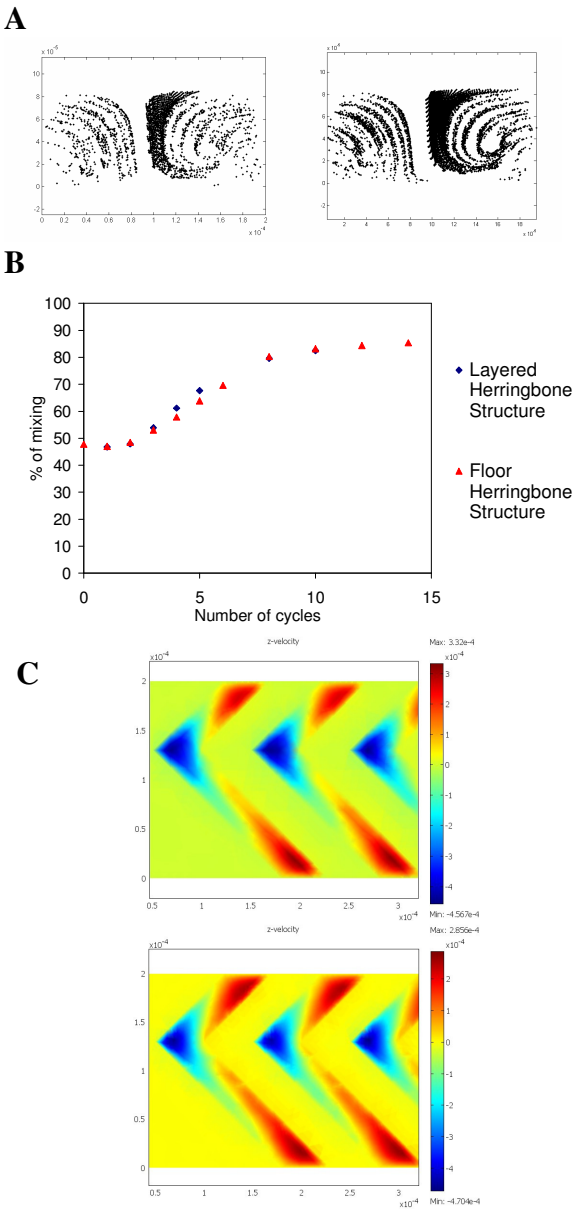

Figure 2. A) Cross-sectional particle distribution profiles after 5 cycles for the layered herringbone (left) and the standard floor herringbone structure (right). B) Percentage of mixing calculated via the nearest neighbour analysis. C) z-velocity at the top channel/groove interface (x-y plane) for the layered (top) and the floor herringbone configuration (bottom).

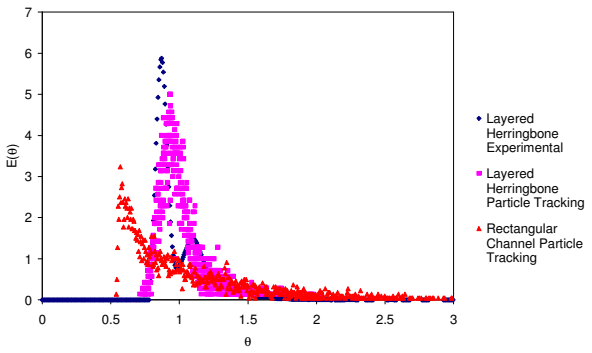

Figure 3. Experimental and numerical RTD for the layered herringbone configuration and comparison with a rectangular channel. For channel dimensions see table 1.

Figure 4 shows two cross-sectional pictures, one at the entrance of the herringbone section, and the other after 1.5 cycles. The signal from the top channel is captured clearly by the microscope. On the other hand, the signal from the bottom channel is weak, as if there was no dye. This was thought to be evidence of flow maldistribution. However, in a following experiment (not shown), the chip was completely filled with dye. In those experiments no signal could be obtained from the bottom channel (unless the chip was flipped over). Hence, there seems to be a problem with the quality of the confocal measurements, also evidenced by high fluorescence intensity at intermediate locations, and this is currently under investigation.

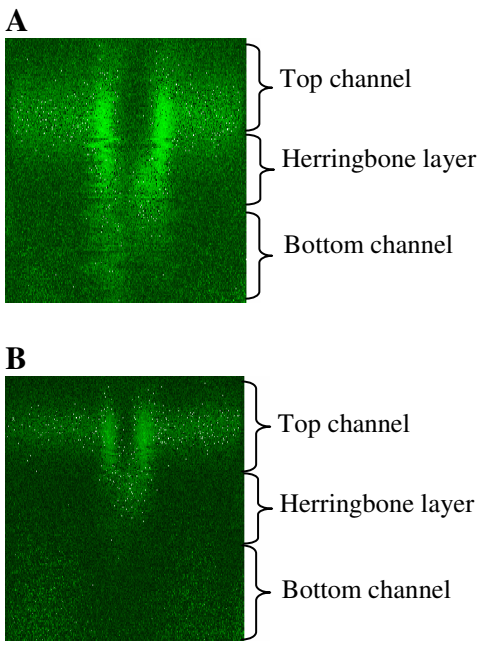

Figure 4. Cross-sectional picture obtained with confocal microscopy. A) Entrance of herringbone section, B) 1.5th cycle.

5. Conclusions

In summary, it was shown that layered herringbone microchannels have a similar behaviour as channels with floor herringbone structures. The two geometries were compared in terms of mixing and residence time distributions. Both herringbone geometries showed similar behaviour for mixing; the layered structure slightly better due to the absence of groove floors. The residence time

distribution for the layered structure was narrower as compared to a rectangular channel. The use of a layered configuration provides the opportunity of having two channels with improved transverse mixing characteristics with a single set of herringbones. This may reduce the microfabrication costs and opens the possibility for new applications where the middle layer can be used both to improve mixing in the bulk, and as a contact area between two different flows.

References

Aubin, J.; Fletcher, D. F.; Xuereb, C. Design of micromixers using CFD modelling. *Chemical Engineering Science* **2005,** *60* (8-9), 2503-2516.

Levenspiel, O.; Turner, J. C. R. Interpretation of Residence-Time Experiments. *Chemical Engineering Science* **1970,** *25* (10), 1605-1609.

Nguyen, N. T.; Wu, Z. G. Micromixers - a review. *Journal of Micromechanics and Microengineering* **2005,** *15* (2), R1-R16.

Pappaert, K.; Biesemans, J.; Clicq, D.; Vankrunkelsven, S.; Desmet, G. Measurements of diffusion coefficients in 1-D micro- and nanochannels using shear-driven flows. *Lab on a Chip* **2005,** *5* (10), 1104-1110.

Stroock, A. D.; Dertinger, S. K.; Ajdari, A.; Mezic, I.; Stone, H. A.; Whitesides, G. M. Chaotic Mixer for Microchannels. *Science* **2002,** *295* (5555), 647-651.